

On the stability of the flow and heat transfer over a moving thin needle with prescribed surface heat flux



Iskandar Waini^{a,b}, Anuar Ishak^{b,*}, Ioan Pop^c

^a *Fakulti Teknologi Kejuruteraan Mekanikal dan Pembuatan, Universiti Teknikal Malaysia Melaka, Hang Tuah Jaya, 76100 Durian Tunggal, Melaka, Malaysia*

^b *School of Mathematical Sciences, Faculty of Science and Technology, Universiti Kebangsaan Malaysia, 43600 UKM Bangi, Selangor, Malaysia*

^c *Department of Mathematics, Babes-Bolyai University, 400084 Cluj-Napoca, Romania*

ARTICLE INFO

Keywords:

Stability analysis
Dual solutions
Thin needle
Surface heat flux

ABSTRACT

The steady flow and heat transfer over a moving thin needle with prescribed surface heat flux is studied. The similarity equations are obtained by using similarity transformation technique. The problem is solved numerically using the boundary value problem solver (bvp4c) in Matlab software. The plots of the skin friction coefficient and the local Nusselt number as well as the velocity and temperature profiles are presented and their behaviors are discussed for different values of the needle size and the velocity ratio parameter. Results show that the decreasing of the needle size enhance the skin friction coefficient and the local Nusselt number on the needle surface. It is found that dual solutions exist (upper and lower branches) for a certain range of the velocity ratio parameter. A stability analysis of the solutions are performed and it shows that the upper branch solution is stable, while the lower branch solution is unstable.

1. Introduction

Due to the importance of various industrial and technological applications, the studies of flow and heat transfer over a moving thin needle have been examined by the researchers with different flow conditions. Some of the applications are hot wire anemometer or shielded thermocouple for measuring the velocity of the wind, microscale cooling devices for heat removal application, microstructure electronic devices which leading to high compactness and effectiveness, etc. The term thin needle is defined as a parabolic revolution about its axes direction in addition to the variable thickness. The motion of the thin needle distracts from the free stream direction, and this situation is the main concern in experimental studies for the flow and heat transfer analysis in order to measure the velocity and temperature profiles of the system.

The first problem on the momentum boundary layer flow over a thin needle in viscous fluid has been studied by Lee [1]. According to Lee [1], as the thickness of the needle goes to zero, the displacement thickness and drag per unit length diminish very slowly, but eventually become zero as the needle vanishes. Then, this work was extended by Narain and Uberoi [2–4] to forced, free and mixed convection flows. Since then, many authors have actively involved in solving the problem of boundary layer flows over thin needles in viscous fluid by considering various aspects such as Cebeci and Na [5], Chen and Smith [6], Wang [7], Kafoussias [8], Ishak et al. [9], and Ahmad et al. [10]. Ishak et al. [9] have investigated the flow over a continuously moving thin needle in a parallel free stream with heat transfer by solving the boundary layer equations using the Keller-box method. They found that there exist dual solutions when the needle and the free stream move in the opposite directions.

* Corresponding author.

E-mail address: anuar_mi@ukm.edu.my (A. Ishak).

<https://doi.org/10.1016/j.cjph.2019.06.008>

Received 29 November 2018; Received in revised form 3 May 2019; Accepted 9 June 2019

Available online 12 June 2019

0577-9073/ © 2019 The Physical Society of the Republic of China (Taiwan). Published by Elsevier B.V. All rights reserved.

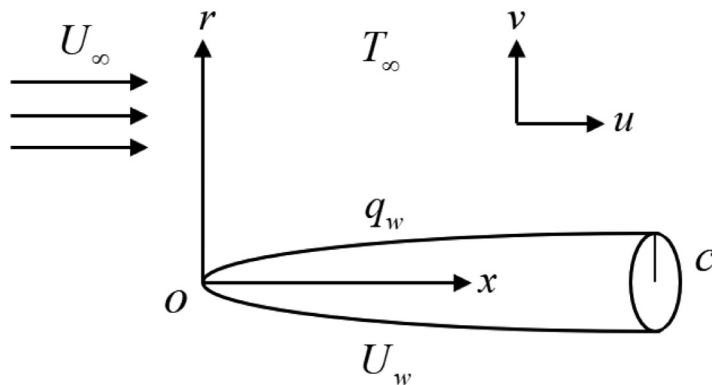


Fig. 1. Physical models and coordinate systems.

Grosan and Pop [11] studied the forced convection boundary layer flow and heat transfer past a horizontal thin needle in a nanofluid with variable wall temperature. They found that the solid volume fraction affects the fluid flow and heat transfer characteristics. Starting from that, many investigations involving nanofluid over a thin needle were carried out by the researchers such as Trimbilas et al. [12], Hayat et al. [13], Ahmad et al. [14], Sk et al. [15], Krishna, et al. [16], Sulochana et al. [17,18], Afridi and Qasim [19], Khan et al. [20], Soid et al. [21] and Salleh et al. [22].

The present study may be regarded as the extension of the paper by Ishak et al. [9], but with the different surface heating condition which is prescribed surface heat flux. In the work of Ishak et al. [9], the case of a prescribed surface temperature was considered. In the present paper, a stability analysis of the dual solutions is also performed to identify which solutions are stable and thus physically reliable when time passes. The partial differential equations governing the fluid flow and the fluid temperature are reduced to a system of ordinary differential equations by using similarity transformation. The system of the equations then is solved numerically using the boundary value problem solver (bvp4c) in Matlab software. The effects of the needle size and the velocity ratio parameter on the flow and heat transfer characteristics are presented in graphical form. To validate the numerical results obtained, comparison is made with the existing results available in the literature for certain special cases.

2. Mathematical formulation

Consider a two-dimensional boundary layer flow over a moving thin needle in a viscous and incompressible fluid. Fig. 1 illustrates the horizontal thin needle whose radius is given by $r = R(x)$ where x and r are the axial and radial coordinates, respectively. The needle is considered thin when its thickness does not exceed that of the boundary layer over it. Thus, the effect of its transverse curvature is important but the pressure gradient along the body may be neglected [1]. Further, it is assumed that the thin needle is subjected to a prescribed surface heat flux. The thin needle moves with a constant velocity, U_w in the same or opposite direction to the constant free stream velocity, U_∞ . Under these assumptions, the boundary layer equations take the following form of cylindrical coordinates (see Chen and Smiths [6], Ishak et al. [9]),

$$\frac{\partial(ru)}{\partial x} + \frac{\partial(rv)}{\partial r} = 0 \tag{1}$$

$$u \frac{\partial u}{\partial x} + v \frac{\partial u}{\partial r} = \nu \frac{\partial}{\partial r} \left(r \frac{\partial u}{\partial r} \right) \tag{2}$$

$$u \frac{\partial T}{\partial x} + v \frac{\partial T}{\partial r} = \frac{\alpha}{r} \frac{\partial}{\partial r} \left(r \frac{\partial T}{\partial r} \right) \tag{3}$$

subject to the boundary conditions,

$$\begin{aligned} u &= U_w, \quad v = 0, \quad \frac{\partial T}{\partial r} = -\frac{q_w}{k} \text{ at } r = R(x) \\ u &\rightarrow U_\infty, \quad T \rightarrow T_\infty \text{ as } r \rightarrow \infty \end{aligned} \tag{4}$$

where u and v are the velocity components along the x - and r -axes, respectively, T is the fluid temperature, ν is the kinematic viscosity, α is the thermal diffusivity, q_w is the surface heat flux, and k is the thermal conductivity.

To obtain similarity solutions for the system of Eqs. (1)–(3) subject to the boundary conditions (4), we introduce the relevant similarity transformation as follows (see Chen and Smiths [6], Ishak et al. [9]),

$$\psi = \nu x f(\eta), \quad \eta = \frac{Ur^2}{\nu x}, \quad \theta(\eta) = \frac{k(T - T_\infty)}{q_w} \left(\frac{4cU}{\nu x} \right)^{1/2} \tag{5}$$

Here, ψ is the stream function that satisfies Eq. (1), and the velocity components are defined as $u = r^{-1} \partial \psi / \partial r$ and $v = -r^{-1} \partial \psi / \partial x$,

respectively. The surface of constant $\eta = c$ corresponds to the surface of revolution and refers to the wall of the needle. Setting $\eta = c$ in Eq. (5) depicts the size and shape of the needle $r = R(x)$ with its surface is given by,

$$R(x) = \left(\frac{\nu cx}{U}\right)^{1/2} \tag{6}$$

Employing the similarity transformation (5), Eqs. (2) and (3) reduce to the following nonlinear ordinary differential equations:

$$2\eta f''' + 2f'' + ff'' = 0 \tag{7}$$

$$\frac{2}{Pr}\eta\theta'' + \frac{2}{Pr}\theta' + f\theta' - \frac{1}{2}f'\theta = 0 \tag{8}$$

and the boundary conditions (4) become,

$$\begin{aligned} f(c) &= \frac{\lambda}{2}c, & f'(c) &= \frac{\lambda}{2}, & \theta'(c) &= -1 \\ f'(\eta) &\rightarrow \frac{1-\lambda}{2}, & \theta(\eta) &\rightarrow 0 & \text{as } \eta &\rightarrow \infty \end{aligned} \tag{9}$$

where primes denote differentiation with respect to η , $Pr = \nu/\alpha$ is the Prandtl number and $\lambda = U_w/U$ is the velocity ratio parameter between the needle and the composite velocity with $U = U_w + U_\infty \neq 0$. It is notice that $\lambda = 0$ and $\lambda = 1$ correspond to a fixed needle in a moving fluid (Blasius flow) and a moving needle in a quiescent fluid (Sakiadis flow), respectively.

The case $0 < \lambda < 1$ is when the needle and the fluid move in the same direction. If $\lambda < 0$, the free stream is directed towards the positive x -direction, while the needle moves towards the negative x -direction. When $\lambda > 1$, the free stream is directed towards the negative x -direction, while the needle moves towards the positive x -direction. In this paper we only consider the case $\lambda \leq 1$, meaning that the direction of the free stream is always towards the positive x -direction.

The physical quantities of interest are the skin friction coefficient C_f or shear stress and the local Nusselt number Nu_x , which are defined as

$$C_f = \frac{\tau_w}{\rho U^2/2}, \quad Nu_x = \frac{xq_w}{k(T_w - T_\infty)} \tag{10}$$

where τ_w is the surface shear stress and q_w is the surface heat flux, which are given by

$$\tau_w = \mu \left(\frac{\partial u}{\partial r}\right)_{r=R(x)}, \quad q_w = -k \left(\frac{\partial T}{\partial r}\right)_{r=R(x)} \tag{11}$$

Using the similarity transformation (5), one obtains

$$C_f Re_x^{1/2} = 8c^{1/2}f''(c) \quad ; \quad Nu_x Re_x^{-1/2} = 2c^{1/2} \left(\frac{1}{\theta(c)}\right) \tag{12}$$

where $Re_x = Ux/\nu$ is the local Reynolds number.

3. Stability analysis

It is noticed that there exist dual solutions of Eqs. (7) and (8) subject to the boundary conditions (9) for a certain range of the velocity ratio parameter λ . Therefore, a stability analysis is performed to determine which solution is stable and thus physically reliable when time passes. According to Merkin [23], the lower branch solutions are unstable and not physically reliable. Meanwhile, the upper branch solutions are stable and thus physically reliable. The same trend was reported by the researchers such as Soid et al. [21,24,25], Salleh et al. [22], Weidman et al. [26], Rosca and Pop [27] Harris et al. [28], Lok et al. [29] and Nasir et al. [30].

To test the temporal stability of the solutions, we need to consider the unsteady case of Eqs. (2) and (3) by introducing the new dimensionless time variable, τ . Note that τ is associated with an initial value problem that is consistent with the solution that will be obtained in practice. The new governing equations for the unsteady state flow are given as

$$\frac{\partial u}{\partial t} + u \frac{\partial u}{\partial x} + v \frac{\partial u}{\partial r} = \frac{\nu}{r} \frac{\partial}{\partial r} \left(r \frac{\partial u}{\partial r} \right) \tag{13}$$

$$\frac{\partial T}{\partial t} + u \frac{\partial T}{\partial x} + v \frac{\partial T}{\partial r} = \frac{\alpha}{r} \frac{\partial}{\partial r} \left(r \frac{\partial T}{\partial r} \right) \tag{14}$$

where t denotes the time while Eq. (1) holds. The new dimensionless variables are introduced based on Eq. (5) as follows:

$$f(\eta, \tau) = \frac{\psi}{\nu x}, \quad \eta = \frac{Ur^2}{\nu x}, \quad \theta(\eta, \tau) = \frac{k(T - T_\infty)}{q_w} \left(\frac{4cU}{\nu x}\right)^{1/2}, \quad \tau = \frac{2Ut}{x} \tag{15}$$

where τ is the dimensionless time. Substituting Eq. (15) into Eqs. (13) and (14) yields,

$$2\eta \frac{\partial^3 f}{\partial \eta^3} + 2 \frac{\partial^2 f}{\partial \eta^2} + f \frac{\partial^2 f}{\partial \eta^2} - \frac{\partial^2 f}{\partial \eta \partial \tau} = 0 \tag{16}$$

$$\frac{2}{Pr} \eta \frac{\partial^2 \theta}{\partial \eta^2} + \frac{2}{Pr} \frac{\partial \theta}{\partial \eta} + f \frac{\partial \theta}{\partial \eta} - \frac{1}{2} \frac{\partial f}{\partial \eta} \theta - \frac{\partial \theta}{\partial \tau} = 0 \tag{17}$$

subjected to the boundary conditions

$$f(c, \tau) = \frac{\lambda}{2}c, \quad \frac{\partial f}{\partial \eta}(c, \tau) = \frac{\lambda}{2}, \quad \frac{\partial \theta}{\partial \eta}(c, \tau) = -1$$

$$\frac{\partial f}{\partial \eta}(\eta, \tau) \rightarrow \frac{1-\lambda}{2}, \quad \theta(\eta, \tau) \rightarrow 0 \quad \text{as } \eta \rightarrow \infty \tag{18}$$

Following [21–30], we test the stability of the dual solutions by perturbing the steady solution $f_0(\eta)$ and $\theta_0(\eta)$ according to,

$$f(\eta, \tau) = f_0(\eta) + e^{-\gamma\tau}F(\eta), \quad \theta(\eta, \tau) = \theta_0(\eta) + e^{-\gamma\tau}G(\eta) \tag{19}$$

where γ is an unknown eigenvalue and functions $F(\eta)$ and $G(\eta)$ are smaller relative to $f_0(\eta)$ and $\theta_0(\eta)$ respectively. We take perturbation in exponential form since it will increase or decrease more rapidly compared to the power functions.

Substituting Eq. (19) into Eqs. (16) and (17), we obtain the following linearized eigenvalue problem:

$$2\eta F'' + 2F'' + f_0 F'' + f_0' F + \gamma F' = 0 \tag{20}$$

$$\frac{2}{Pr} \eta G'' + \frac{2}{Pr} G' + f_0 G' + \theta_0' G - \frac{1}{2} f_0' G - \frac{1}{2} F' \theta_0 + \gamma G = 0 \tag{21}$$

along with the boundary conditions

$$F(c) = 0, \quad F'(c) = 0, \quad G'(c) = 0$$

$$F'(\eta) \rightarrow 0, \quad G(\eta) \rightarrow 0 \quad \text{as } \eta \rightarrow \infty \tag{22}$$

We solve the eigenvalue problem (20)–(22) and the solutions obtained give an infinite number of eigenvalues ($\gamma_1 < \gamma_2 < \gamma_3 < \dots$) of the solutions of Eqs. (7)–(9). If the smallest eigenvalue is positive, there is an initial decay which is the flow is stable. Besides, there is an initial growth of disturbance if the smallest eigenvalue is negative which mean the flow is unstable, as time passes.

4. Results and discussion

The nonlinear ordinary differential Eqs. (7) and (8) along with the boundary conditions (9) were solved numerically using the boundary value problem solver (bvp4c) in Matlab software. The function bvp4c applies the finite difference scheme, where the solution can be obtained using an initial guess supplied at an initial mesh point and changes step size to get the specified accuracy. This method implements the three-stage Labatto IIIa formula and collocation code. The details of this method can be found in Shampine et al. [31]. The suitable initial guess and the boundary layer thickness η_∞ must be chosen depending on the values of the parameters used. To solve these boundary value problems, it is necessary to first reduce the equations to a system of first order ordinary differential equations.

Comparative study of the skin friction coefficient $f''(c)$ with the numerical results of Ishak et al. [9] and Soid et al. [21] for several values of the needle size c is carried out to validate the numerical results obtained. The comparison shows a favorable agreement, as can be seen in Table 1. This gives us strong confidence that the present results are correct and accurate. On the other hand, the values of the local Nusselt number $1/\theta(c)$ for the case of the prescribe heat flux when $Pr = 1$ are shown in Table 2. From Table 2, we can observe that the local Nusselt number $1/\theta(c)$ is decreasing with the increasing of the needle size c and the decreasing of velocity ratio parameter λ for the upper branch.

Figs. 2 and 3 display the effects of the needle size c and the velocity ratio parameter λ on the variation of the skin friction coefficient $f''(c)$ and the local Nusselt number $1/\theta(c)$, respectively. From these figures, it can be observed that the decreasing of the

Table 1
Values of the skin friction coefficient $f''(c)$.

c	$\lambda = 0$			$\lambda = -1$					
	Ishak et al. [9]	Soid et al. [21]	Present Results	Ishak et al. [9]		Soid et al. [21]		Present Results	
				First Solution	Second Solution	First Solution	Second Solution	First Solution	Second Solution
0.01	8.4924	8.491454	8.491455	26.6021	2.8031	26.599394	2.805533	26.599394	2.809340
0.1	1.2888	1.288778	1.288778	3.7162	0.3884	3.703713	0.389103	3.703714	0.388454
0.2		0.751665	0.751665			2.005424	0.227837	2.005427	0.227655
0.3			0.552377					1.377147	0.171510

Table 2
Values of the local Nusselt number $1/\theta(c)$ when $Pr = 1$.

λ	$c = 0.1$		$c = 0.2$	
	First Solution	Second Solution	First Solution	Second Solution
1	3.013943	–	1.876869	–
0.5	2.971771	–	1.806276	–
0	2.879977	–	1.694600	–
–1	2.617342	–91.507374	1.398291	–4.719336

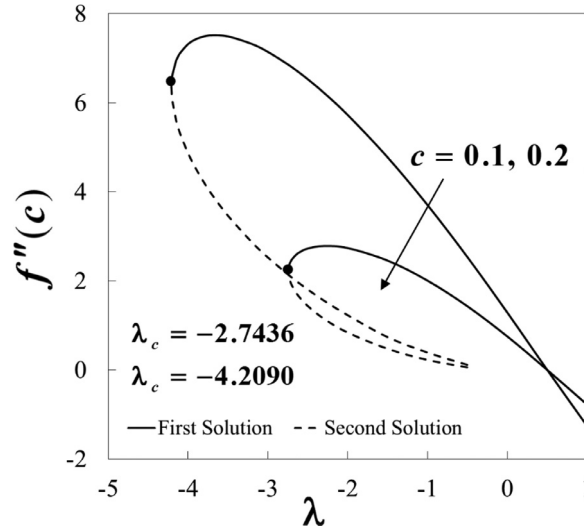


Fig. 2. Variation of skin friction coefficient $f''(c)$ with λ for various values of c .

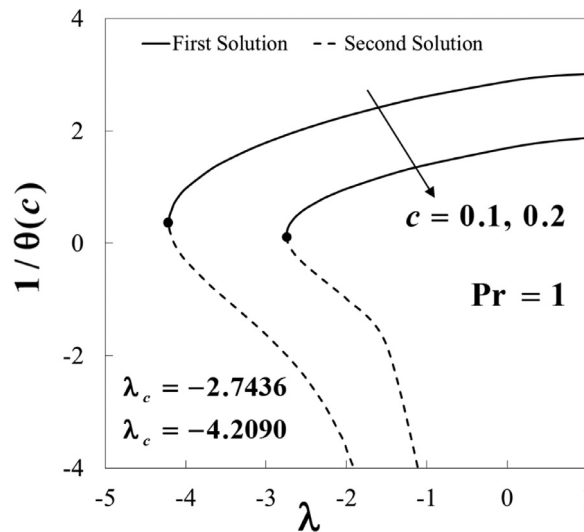


Fig. 3. Variation of the local Nusselt number $1/\theta(c)$ with λ for various values of c when $Pr = 1$.

needle size enhance the values of the skin friction coefficient and the local Nusselt number on the needle surface. This implies that the contact of the needle surface with the fluid particle is decreasing if the needle size is getting smaller. This leads to the reduction of the drag force that occurs on the needle surface and the fluid flow. Meanwhile, the decreasing of the needle size will cause the heat transfer to accelerate since the heat is easily diffused through a thin surface rather than a thick surface.

From Fig. 3, it is showed that $1/\theta(c)$ decreases as λ changes from positive to negative values for the upper branch. The local Nusselt number $1/\theta(c)$ decreases due to increasing value of the surface temperature $\theta(c)$. This result is consistent with the result of the

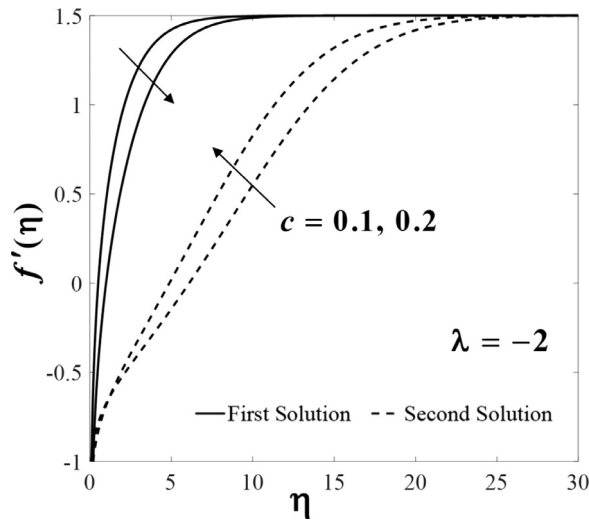


Fig. 4. The velocity profiles $f'(\eta)$ for $c = 0.1$ and $c = 0.2$ when $\lambda = -2$.

skin friction coefficient presented in Fig. 2. However, for the lower branch $1/\theta(c)$ increases with the decreasing value of λ . Further from Fig. 2, it can be seen that unique solution is obtained for $\lambda \geq 0$ where the needle and the free stream move in the same direction. Meanwhile, dual solutions exist for the negative value of λ when the needle and the free stream move in the opposite directions. Also, it is observed that for $\lambda > 0.5$ the value of $f''(c)$ is negative then become zero when $\lambda = 0.5$. The zero value of $f''(c)$ when $\lambda = 0.5$ corresponds to the equal velocity of the needle and the free stream. The existence of dual solutions depends on the values of λ . The plots of $f''(c)$ vs c and $1/\theta(c)$ vs c will show this non-unique solution if the right values of λ are chosen. Figs. 2 and 3 show the range of λ where dual solutions are possible.

The solutions bifurcate at the critical value λ_c as shown in Fig. 2. No solution is obtained for $\lambda < \lambda_c$. Based on our computations, the critical value of λ for the needle size $c = 0.1$ is $\lambda_c = -4.2090$, meanwhile $\lambda_c = -2.7346$ for the needle size $c = 0.2$. The range of λ for which the solution is in existence increase as the needle size decreases. There is no similarity solutions exist beyond this critical value due to the breakdown of the boundary layer approximations. According to Lee [1], as the thickness of the needle goes to zero, the displacement thickness and drag per unit length diminish very slowly, but eventually become zero as the needle vanishes.

The velocity and temperature profiles for different values of the needle size c when $Pr = 1$ and $\lambda = -2$ are plotted in Figs. 4 and 5, respectively. These figures show that there exist two different profiles for a particular value of the velocity ratio parameter λ . It is found that the decreasing of the needle size leads to the increment of the fluid velocity for the upper branch, while it decreases for the lower branch. Physically, the thinner surface of the needle leads to the decrease in the drag force that occurs between the needle and the fluid particles in the flow. Note that the reduction in the needle size could retard the velocity boundary layer thickness for the upper branch. Fig. 5 shows that the fluid temperature and thermal boundary layer decreases for the upper branch, while it is increases

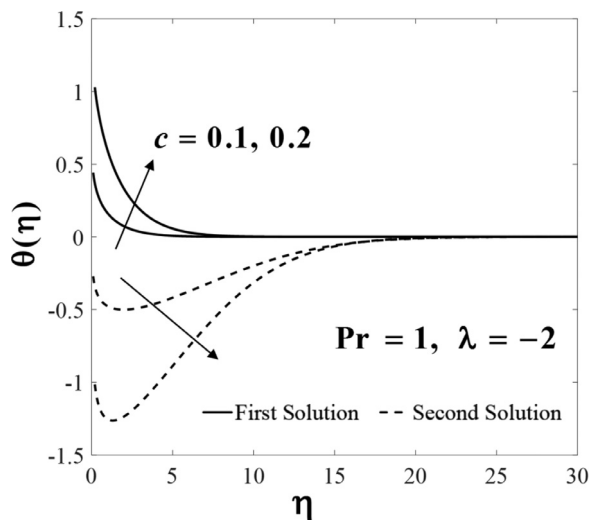


Fig. 5. The temperature profiles $\theta(\eta)$ for $c = 0.1$ and $c = 0.2$ when $Pr = 1$ and $\lambda = -2$.

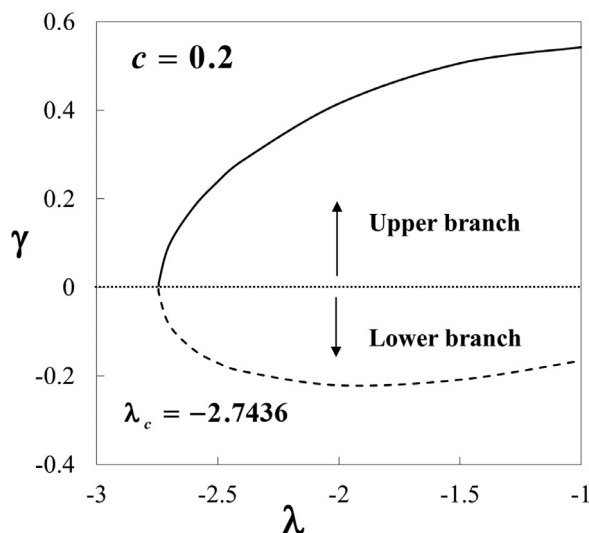


Fig. 6. Smallest eigenvalues γ for various values of λ when $c = 0.2$.

for the lower branch with the decreasing of the needle size. Moreover, there are regions within the thermal boundary layer where $\theta(0) < 0$ as shown in Fig. 5. This result seems to contradict the second law of thermodynamics. This is due to the fact that the second solution is unstable and not physically reliable. Based on Figs. 4 and 5, all profiles obtained have fulfilled the requirement of the far field boundary condition (9) asymptotically, which supports the validity of the numerical results obtained.

Fig. 6 shows the plot of the smallest eigenvalue γ for different values of the velocity ratio parameter λ when $c = 0.2$. Similar result is obtained for $c = 0.1$, but with smaller range of λ . This figure indicates that the negative value of γ refers to an initial growth of disturbance, and the flow is in unstable mode. Meanwhile, the positive value of γ denotes an initial decay of disturbance, and the flow is said to be in a stable mode. From this figure, as the values of λ approaching λ_c , the smallest eigenvalue γ tends to zero either from the upper branch or the lower branch solution. This shows that the transitions from positive (stable) to negative (unstable) of γ occur at the turning (bifurcation) points.

5. Conclusions

The problem of steady flow and heat transfer over a moving thin needle with prescribed surface heat flux was investigated. This study was based on the assumption that the needle moves in the same or opposite directions to the free stream. For the conclusion, the enhancement of the skin friction coefficient and the local Nusselt number (heat transfer rate) at the needle surface were observed, as the needle size is getting smaller. Dual solutions were found for the case when the needle and the free stream move in the opposite directions, while the solution is unique when they move in the same direction. A stability analysis was conducted to determine the stability of the dual solutions. It was found that only one of the solution is stable when time passes, while the other is unstable and thus not physically reliable in a long run.

Conflict of interest

None.

Acknowledgements

The authors wish to express their thanks to the Reviewers for their constructive comments and suggestions. The financial supports received from the Universiti Kebangsaan Malaysia (Project Code: GUP-2018-153), Universiti Teknikal Malaysia Melaka and the Ministry of Education, Malaysia are gratefully acknowledged. The work of Ioan Pop was supported by the grant PN-III-P4-ID-PCE-2016-0036, UEFISCDI from the Romanian Ministry of Science.

Supplementary materials

Supplementary material associated with this article can be found, in the online version, at doi:[10.1016/j.cjph.2019.06.008](https://doi.org/10.1016/j.cjph.2019.06.008).

References

- [1] L.L. Lee, Boundary layer over a thin needle, *Phys. Fluids*. 10 (1967) 820–822.

- [2] J.P. Narain, M.S. Uberoi, Forced heat transfer over thin needles, *J. Heat Transfer*. 94 (1972) 240–242.
- [3] J.P. Narain, M.S. Uberoi, Combined forced and free-convection heat transfer from vertical thin needles in a uniform stream, *Phys. Fluids*. 15 (1972) 1879–1882.
- [4] J.P. Narain, M.S. Uberoi, Combined forced and free-convection over thin needles, *Int. J. Heat Mass Transf.* 16 (1973) 1505–1512.
- [5] T. Cebeci, T.Y. Na, Laminar free-convection heat transfer from a needle, *Phys. Fluids*. 12 (1969) 463–465.
- [6] J.L.S. Chen, T.N. Smith, Forced convection heat transfer from nonisothermal thin needles, *J. Heat Transfer* 100 (1978) 358–362.
- [7] C.Y. Wang, Mixed convection on a vertical needle with heated tip, *Phys. Fluids A: Fluid Dyn.* 2 (1990) 622–625.
- [8] N.G. Kafoussias, Mixed free convection and mass transfer flow along a vertical needle, *Int. J. Energy Res.* 16 (1992) 43–49.
- [9] A. Ishak, R. Nazar, I. Pop, Boundary layer flow over a continuously moving thin needle in a parallel free stream, *Chin. Phys. Lett.* 24 (2007) 2895–2897.
- [10] S. Ahmad, N.M. Arifin, R. Nazar, I. Pop, Mixed convection boundary layer flow along vertical thin needles: assisting and opposing flows, *Int. Commun. Heat Mass Transf.* 35 (2008) 157–162.
- [11] T. Grosan, I. Pop, Forced convection boundary layer flow past nonisothermal thin needles in nanofluids, *J. Heat Transfer* 133 (2011) 054503.
- [12] R. Trimbitas, T. Grosan, I. Pop, Mixed convection boundary layer flow along vertical thin needles in nanofluids, *Int. J. Numer. Methods Heat Fluid Flow*. 24 (2014) 579–594.
- [13] T. Hayat, M.I. Khan, M. Farooq, T. Yasmeen, A. Alsaedi, Water-carbon nanofluid flow with variable heat flux by a thin needle, *J. Mol. Liq.* 224 (2016) 786–791.
- [14] R. Ahmad, M. Mustafa, S. Hina, Buongiorno's model for fluid flow around a moving thin needle in a flowing nanofluid: a numerical study, *Chin. J. Phys.* 55 (2017) 1264–1274.
- [15] M.T. Sk, K. Das, P.K. Kundu, Consequences of nanoparticle diameter and solid-liquid interfacial layer on the SWCNT/EO nanofluid flow over various shaped thin slendering needles, *Chin. J. Phys.* 56 (2018) 2439–2447.
- [16] P.M. Krishna, R.P. Sharma, N. Sandeep, Boundary layer analysis of persistent moving horizontal needle in blasius and sakiadis magnetohydrodynamic radiative nanofluid flows, *Nucl. Eng. Technol.* 49 (2017) 1654–1659.
- [17] C. Sulochana, G.P. Ashwinkumar, N. Sandeep, Joule heating effect on a continuously moving thin needle in MHD sakiadis flow with thermophoresis and brownian moment, *Eur. Phys. J. Plus.* 132 (2017) 387.
- [18] C. Sulochana, S.P. Samrat, N. Sandeep, Boundary layer analysis of an incessant moving needle in MHD radiative nanofluid with joule heating, *Int. J. Mech. Sci.* 128–129 (2017) 326–331.
- [19] M.I. Afridi, M. Qasim, Entropy generation and heat transfer in boundary layer flow over a thin needle moving in a parallel stream in the presence of nonlinear rosseland radiation, *Int. J. Therm. Sci.* 123 (2018) 117–128.
- [20] M.W.A. Khan, M.I. Khan, T. Hayat, A. Alsaedi, Entropy generation minimization (EGM) of nanofluid flow by a thin moving needle with nonlinear thermal radiation, *Physica B: Condensed Matter* 534 (2018) 113–119.
- [21] S.K. Soid, A. Ishak, I. Pop, Boundary layer flow past a continuously moving thin needle in a nanofluid, *Appl. Therm. Eng.* 114 (2017) 58–64.
- [22] S.N.A. Salleh, N. Bachok, N.M. Arifin, F.M. Ali, I. Pop, Stability analysis of mixed convection flow towards a moving thin needle in nanofluid, *Appl. Sci.* 8 (2018) 195 842.
- [23] J.H. Merkin, Mixed convection boundary layer flow on a vertical surface in a saturated porous medium, *J. Eng. Math.* 14 (1980) 301–313.
- [24] S.K. Soid, A. Ishak, I. Pop, Unsteady MHD flow and heat transfer over a shrinking sheet with ohmic heating, *Chin. J. Phy.* 55 (2017) 1626–1636.
- [25] S.K. Soid, A. Ishak, I. Pop, MHD flow and heat transfer over a radially stretching/shrinking disk, *Chin. J. Phy.* 56 (2018) 58–66.
- [26] P.D. Weidman, D.G. Kubitschek, A.M.J. Davis, The effect of transpiration on self-similar boundary layer flow over moving surfaces, *Int. J. Eng. Sci.* 44 (2006) 730–737.
- [27] A.V. Roşca, I. Pop, Flow and heat transfer over a vertical permeable stretching/shrinking sheet with a second order slip, *Int. J. Heat Mass Transf.* 60 (2013) 355–364.
- [28] S.D. Harris, D.B. Ingham, I. Pop, Mixed convection boundary-layer flow near the stagnation point on a vertical surface in a porous medium: brinkman model with slip, *Transp. Porous Media.* 77 (2009) 267–285.
- [29] Y.Y. Lok, A. Ishak, I. Pop, Oblique stagnation slip flow of a micropolar fluid towards a stretching/shrinking surface: a stability analysis, *Chin. J. Phy.* 56 (2018) 3062–3072.
- [30] N.A.A. Nasir, A. Ishak, I. Pop, Stagnation-point flow and heat transfer past a permeable quadratically stretching/shrinking sheet, *Chin. J. Phy.* 55 (2017) 2081–2091.
- [31] L.F. Shampine, I. Gladwell, S. Thompson, *Solving ODEs With MATLAB*, Cambridge University Press, Cambridge, 2003.